Effect of Rolling Speed on the Exit Cross Sectional Shape in Rod Rolling Process

Youngseog Lee[1,#]

1 Department of Mechanical Engineering, Chung-Ang University, Seoul 156-756, Korea
Corresponding Author / E-mail: ysl@cau.ac.kr, TEL: +82-2-820-5256, FAX: +82-2-814-9476

KEYWORDS : Hot rod rolling, Maximum spread, Rolling speed, Exit cross sectional shape

A rolling speed dependent spread model is proposed for predicting the exit cross sectional shape in oval-round (or round-oval) pass rod rolling process when the rolling speed is very high. The effect of rolling speed on the exit cross sectional shape is measured by performing a four-pass continuous high speed (~80m/s) rod rolling test and is described in terms of the spread correction parameter. The validity of the model is examined by applying it to rod rolling process at POSCO No. 3 Rod Mill. The cross sectional shapes of workpiece predicted by the proposed model coupled with the surface profile prediction method [6] are in good agreement with those obtained experimentally.

Manuscript received: December 12, 2005 / Accepted: April 24, 2006

NOMENCLATURE

C_x, C_y: Coordinate where the roll groove and workpiece are separated from each other
D: Groove depth
G : Roll gap
H_p: Pass height
R_a: Radius of curvature of incoming workpiece in round-oval pass rolling.
R_g : Radius of curvature of round groove
R_f : Allowable minimum radius of surface profile in oval groove at the exit
R_S: Stress free surface profile at the exit
R_1 : Radius of curvature of oval groove
V_r: Rolling speed
W_i: Width of equivalent rectangular cross section of the incoming (inlet) workpiece
W_f: Maximum spread that the groove can allow
W_{max}: Maximum spread of the outgoing (exit) workpiece
W^c_{max}: Corrected maximum spread of the outgoing (exit) workpiece when rolling speed is higher.
W_t: Weighting function for calculating the stress free surface profile of workpiece
α : Relief angle of round groove

1. Introduction

In continuous hot rod rolling process, materials are processed into rods with acceptable dimensional tolerance as they pass through the rolling stands, with the cross sectional shape of the materials being progressively altered by roll grooves. To predict the exit cross sectional shape of workpiece at a pass (stand), a number of numerical studies that simulate rod rolling were presented on the basis of three-dimensional finite element analysis[1-5]. The FEA is very effective in calculating the cross sectional shape of workpiece together with the distribution of strain, strain rate, temperature and stress but requires at least several hours to run a program for a single pass since three dimensional analysis is required in nature. Furthermore, governing differential equation should consider inertia, i.e., rate effect, on these when the workpiece is deformed at high strain rate.

Thus, considering computational time and complicated boundary conditions including finite element formulation of the rate dependent governing equation, an analytical method with a simple form and reliable accuracy and a non-iterative computational frame has been highly desired if one is interested in the exit cross sectional shape only.

In 1983, Shinokura and Takai[6] proposed a model which predicts the maximum spread of an outgoing (exit) workpiece as a function of roll radius, the geometry of an incoming (inlet) workpiece, and the area fraction between the incoming workpiece and the geometry of roll groove. Then, they suggested the model for predicting the surface profile of exit cross section in an oval pass only. The surface profile, however, was approximated as a curve that consisted of two arcs.

Lee and Choi [7] and Lee and Goldhahn[8], proposed an analytical method for predicting the exit cross sectional shape of workpiece for the oval-round (or round-oval) pass rolling, which is most widely used in the rod mill around world. Note we can obtain the cross sectional shape and area at each pass (stand) if we can compute the stress free surface profile at the exit of rolling. The oval-round rolling means that a workpiece with round cross section is rolled in the oval groove. The round-oval pass rolling is vice versa. The stress free surface profile is referred as the surface profile hereafter for convenience.

The surface profile at the exit is computed using information of the spread of workpiece at the exit, shape of the inlet cross-section and design parameter of the roll groove. In this approach, the spread of workpiece during rolling is assumed as rate independent. The validity of this approach was examined by a series of the round-oval (or oval-round) pass rolling experiment when rolling speed is lower than 0.5m/s.

Capability of the analytical method for the practical rod rolling process where the rolling speed increases up to 80m/s becomes then important. It is well acknowledged that rolling speed affects the spread of workpiece during rolling and subsequently its surface profile. Hence, one must set up a model that takes into account the effect of rolling speed on the spread of workpiece to compute the cross sectional shape correctly. For this purpose, a four-pass high speed rod rolling test was conducted. This test was implemented in cooperation with the Institute for Metal Forming at Technical University Bergakademie, Freiberg, Germany, where appropriate high speed rolling testing facilities are available. A model considering the rolling speed effect on the spread of workpiece has been established and then applied to POSCO No. 3 Rod Mill.

2. Surface profile prediction method – rolling speed independent

The analytical method which predicts the surface profile of the exit cross section of workpiece for the oval-round (or round-oval) pass rolling sequence is robust and non-iterative in computation.[6, 7] The advantage of this method is that only the geometric consideration is required in the formulation. Hence, it greatly simplifies the problem of obtaining the final rolled shape.

2.1 Surface profile in oval-round pass rolling

In oval-round pass rolling, possible surface profiles of workpiece at the exit of rolling is illustrated in Fig. 1. R_l is the radius of curvature of the inlet cross section, R_s is the radius of curvature of the outgoing cross section and R_g is the radius of the round roll groove.

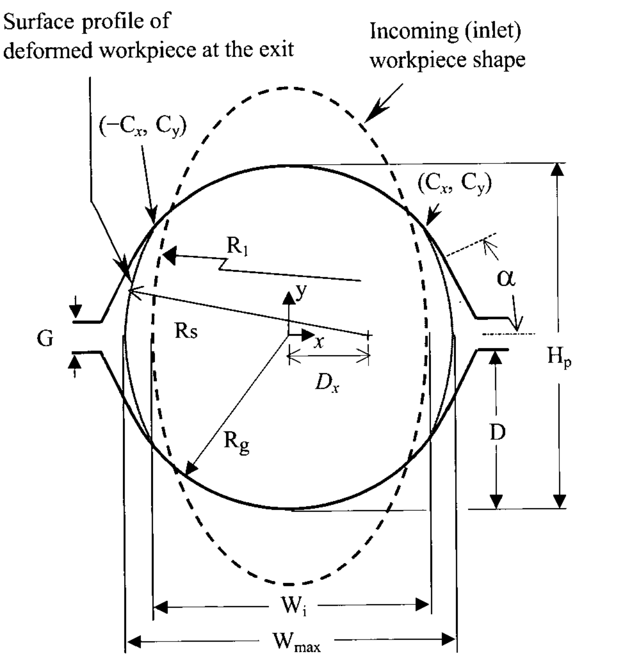

Fig. 1 Geometrical designation of round roll groove and the radius of surface profile, R_S, of a workpiece for the oval-round pass rolling

Assuming that W_{max}, the maximum spread does not exceed $2R_g$, the radius of the surface profile of the exit cross section, R_s, may be given by

$$R_s = R_l \cdot W_t + R_g \cdot (1 - W_t), \tag{1}$$

$$W_t = \frac{2 \cdot R_g - W_{max}}{2 \cdot R_g - W_i} \tag{2}$$

where W_t is a weighting function, W_i is the width of the inlet cross section, and W_{max} is the maximum spread of the exit cross section, which can be calculated by Shinokura and Takai equation.[8] According to Eq. (1), R_s becomes R_l when $W_{max}=W_i$ (no spread at all), and R_s becomes R_g when $W_{max}=2R_g$. It should be noted that Eq. (1) is valid under the condition that $R_g=D_r+G/2$. Once R_s is determined, the point (C_x, C_y), where the roll groove and workpiece are separated each other, can be obtained. The exit cross sectional area may be calculated accordingly. It should be noted that the material is assumed to be incompressible during rolling and only geometric change was considered in the formulation.

2.2. Surface profile in round-oval pass rolling

The geometrical designation of the round-oval pass rolling is described in Fig. 2. R_a is the radius of curvature of the incoming cross section, R_s is the radius of curvature of the outgoing cross section, and R_l is the radius of the oval roll groove.

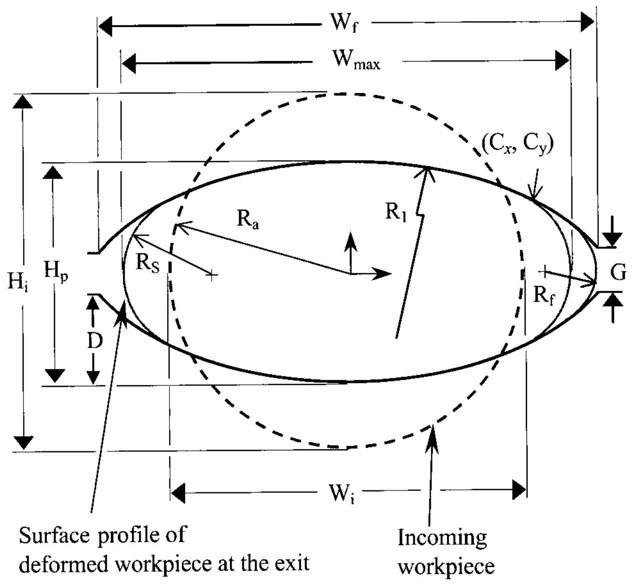

Fig. 2 Geometrical designation of oval roll groove and the radius of the surface profile, R_S, of a workpiece for the round-oval pass rolling

Assuming that W_{max} does not exceed W_f (the width of the roll groove area), an equation similar to Eq. (1) may be proposed for the round-oval pass rolling as follows:

$$R_s = R_a \cdot W_t + R_f \cdot (1 - W_t), \tag{3}$$

$$W_t = \frac{W_f - W_{max}}{W_f - W_i} \tag{4}$$

where R_f is the radius to be achieved when $W_{max}=W_f$. R_f may be approximated by the radius of a circle which is located within the oval roll groove area and passing through the point ($x=W_f/2$, $y=0$). Then, it may be shown that

$$R_f = \frac{R_l H_p - (W_f^2 + H_p^2)/4}{2R_l - W_f}. \tag{5}$$

where H_p is the thickness of the oval roll groove area. Once R_s is determined, the point (C_x, C_y) can be obtained. The area of the exit cross section may be calculated accordingly and the procedure for it is described in details in Ref.[7, 8]

3. High speed rod rolling test

High speed rod rolling test was conducted using four-pass continuous high speed rod rolling facilities in the University of Freiberg, Germany. Fig. 3 illustrates a complete view of the continuous pilot high speed rod rolling mill. It should be noted that TU Bergakademie Freiberg is the only institute in the world with its own continuous and high speedy rod rolling mill. This was built in 1982 after industrial requirements for a special equipped laboratory mill to realise practice relevant rolling tests and other investigations.

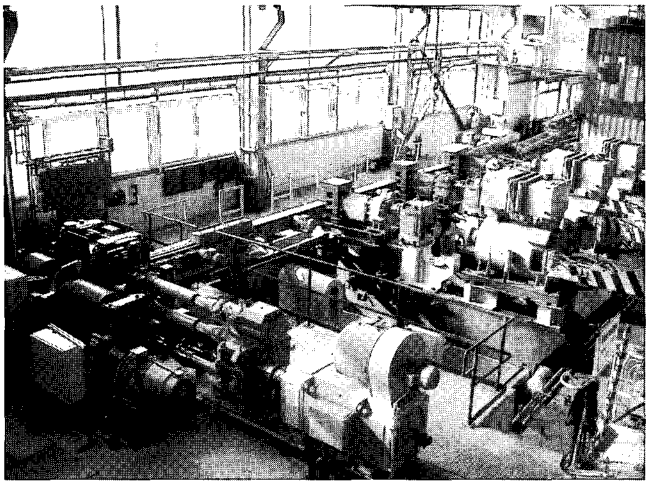

Fig. 3 A complete view of the continuous pilot high speed rod rolling mill in University of Freiberg in Germany

Fig. 4 illustrates the schematic of the four-pass high speed rod rolling test. The stands can be shifted to allow the installation of an integrated cooling section for temperature control within a variety of ranges. The roll forces were measured at each stand (pass) and the surface temperatures of workpiece during rolling are measured before 1st pass, after 2nd pass and after 4th pass. The finishing rolling speed for this study could be varied up to 80m/sec. Initial diameter of specimen (low carbon (0.15%C) steel) is 12mm and diameter of finally rolled specimen is approximately 8mm. Test was repeated twice under the same rolling condition. Test was conducted when the desired temperature (1000^{0}C) in the reheating furnace was reached.

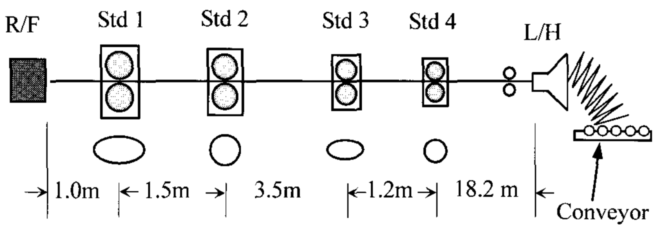

Fig. 4 Schematic for the four-pass high speed rod rolling test and distance between stands. The oval grooves are installed at Std. 1 and 3 and round grooves at Std. 2 and 4. R/F and L/H represents for the reheating furnace and laying head.

After rolled at stand no. 4, the rod travels horizontally to the laying head (cone) where it pass between a driven wheel guide and a roller chain which directs the rod vertically downward through a short and curved "laying" pipe. The bottom end of the pipe revolves rapidly and forms the rod into rings which overlaps in spenserian form as they fall onto the conveyor

Fig. 5 shows the design parameters and roll grooves used in the test. It should be stressed that this four-pass rolling mill consists of horizontal-vertical rolling type and therefore one doesn't need to twist the workpiece after oval pass.

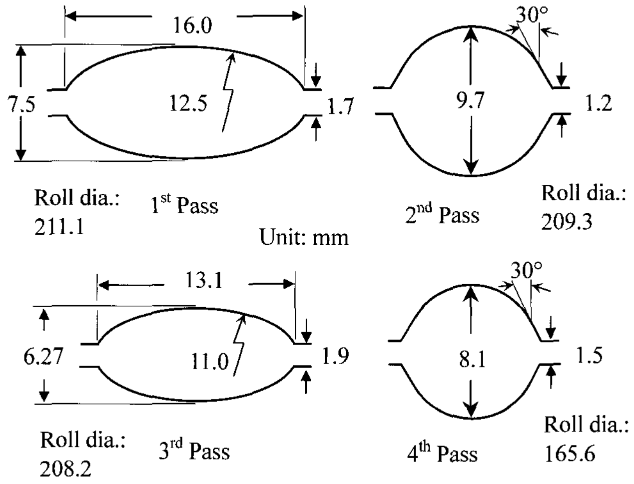

Fig. 5 Design parameters and roll grooves used in the four-pass high speed rolling test

4. Rolling speed dependent maximum spread model

In Fig. 6, spread ratio is obtained experimentally as a function of rolling speed. The spread ratio is defined as the maximum width of outgoing workpiece, W_{max} over the maximum width of incoming workpiece, W_i. It shows the spread ratio decreases almost a linear manner as rolling speed increases. Based on the experimental data, one can derive a expression for the spread ratio-rolling speed relationship as shown in Eq. (6)

$$W^{C}_{\max} = W_{\max}\left[1.0 - \left(\frac{9.1}{100}V_r\right)/100\right] \tag{6}$$

W^c_{max} indicates the spread of workpiece when the rolling speed is greater than 2.0m/s and W_{max} represents maximum spread of workpiece at lower rolling speed (< 2.0m/s). V_r stands for the rolling speed at a stand.

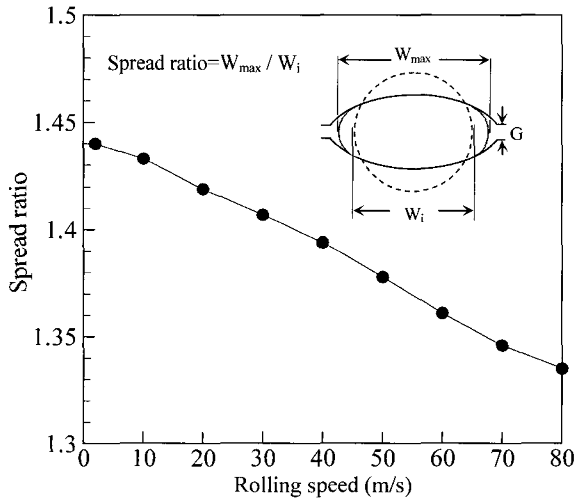

Fig. 6 Correlations between rolling speed and the spread ratio when the rolling speed varies

5. Results and Discussion

Fig. 7 illustrates the predicted and measured surface profiles of workpiece for intermediate finishing stand train and finishing block mill unit of POSCO No. 3 Rod Mill. It has a feature of the horizontal-

horizontal type tandem rolling in the roughing train and horizontal-vertical type one in the finishing train with oval-round (or round-oval) pass sequence, except pass No. 1 (box pass). The rolling line consists of two strands and 29 stands in each strand. Rolling speed of the intermediate finishing stand unit is in the range of 2.5 ~ 11 m/s and that of finishing stand unit (finishing block mill) is 13~80m/s. As stand number increases, the cross sectional area decreases and rolling speed increases.

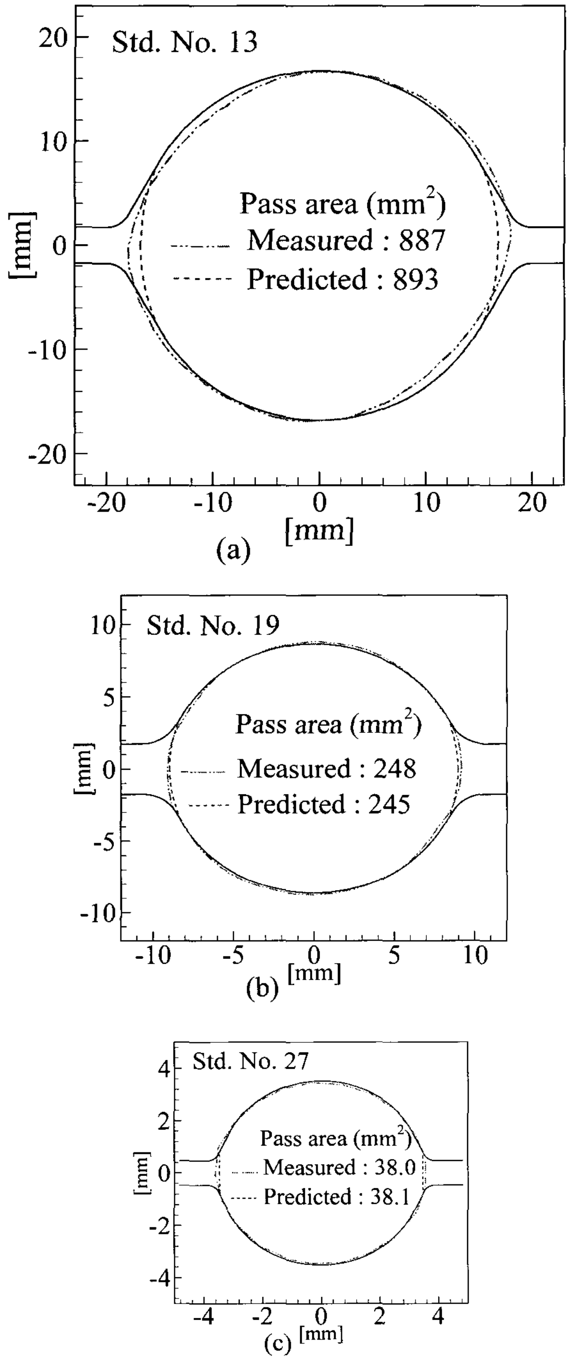

Fig. 7 Predicted and measured surface profile of the workpiece in the intermediate finishing stand unit and finishing block mill unit in POSCO No. 3 Rod Mill. For relative comparison of cross sectional area at each pass (stand), the size of each figure (a, b, c) is different

When an emergency stop caused by an instant blackout in the rod mill took place, the cross sections with 30mm thickness were obtained by cutting the middle part of the workpiece between stands (passes). The cross section of the workpiece was then smoothed by a milling machine. Finally, the coordinates of cross sectional shape were obtained by using the boundary extraction program followed by scanning the cross section of the workpieces.

Solid lines represent the roll groove shape and dashed lines do the predicted surface profile of the exit cross sectional shape. The measured surface profiles are shown by dashed-dot-dot lines, for clarity.

Fig. 7(a) shows the deformed workpiece was somehow rotated during rolling. This is due to unstable rolling attributed to horizontal-horizontal stand type rolling sequence in the roughing train. It should be mentioned that the shapes (roll groove and workpiece cross section) in Fig. 7(b) is not circular even though it is the round pass rolling. This is because the roll gap (i.e., pass height) is reduced to some extent to control the volume flux balance (amount of metal passing through a roll groove per unit time) between stands. Fig. 7(c) illustrates slightly over-filled cross section at the exit. In overall, good agreements were noted between predictions and measurements.

Fig. 8 illustrates the cause of the unstable rolling at the round pass, shown in Fig. 7(a). We may call Fig. 8(a) ‘under-twist rolling’ and Fig. 8(b) ‘over-twist rolling’, depending on the angle of uprightness.

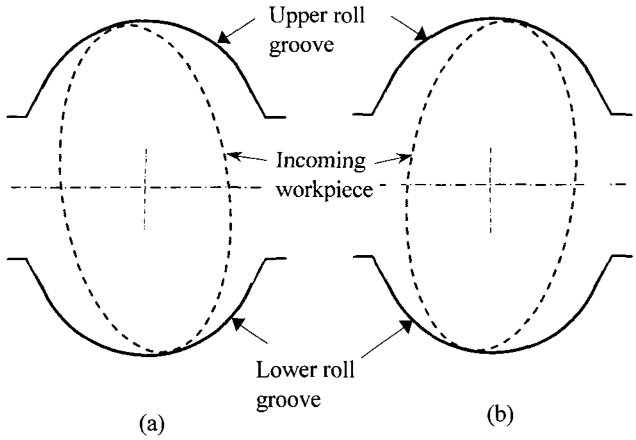

Fig. 8 Incoming workpiece and roll groove in oval-round rolling pass at the very biting position. (front view) (a) Incoming oval shape workpiece is slightly twisted left wise and (b) Incoming oval shape workpiece is slightly twisted right wise

This kind of problem occurs straightforwardly in horizontal-horizontal stand type rolling sequence. It is not easy to control the twister (a device which makes the oval workpiece twisted during interpass transportation) to have incoming workpiece upright as it enters the round roll groove because the wear always occur at inside of the twister and consequently, clearance between workpiece and the inner part of the twister increases. One way to prohibit this problem might be installing a sensing device detecting the uprightness of workpiece at the entry of round groove.

Fig. 9 illustrates the surface profiles at Std. No. 13 when the surface profile prediction method is independent of rolling speed and dependent of rolling speed. It shows the difference is very small since rolling speed at the Std. No. 13 is only 2.98m/s. This implies the rolling speed dependent spread correction factor (Eq. (6)) doesn't contribute remarkably to the calculation of surface profile. Pass area with correction factor is 887mm^2 and that without correction factor is 889mm^2. The difference may increase as rolling speed increases, i.e., the stand number increases. The comparison for the increased rolling speed is not given since the maximum spread of deformed workpiece at Std. No. 19 (11.9m/s) and 27 (66.6m/s) squeezes in the roll gap (G) area (see Figs. 1 and 2) and therefore computation stops. Note the analytical method doesn't work if the deformed workpiece flows into the roll gap region.

6. Conclusions

In the present study, the capability that predicts the surface profile

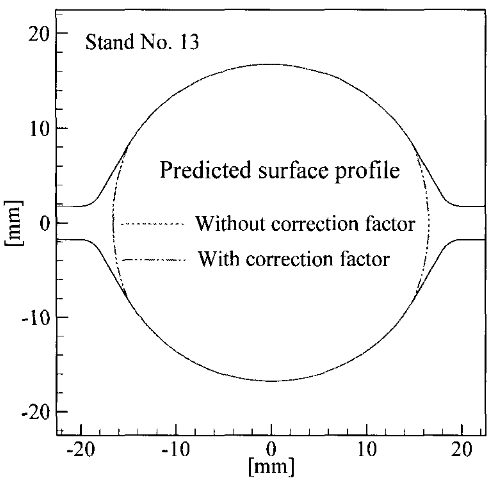

Fig. 9 Comparison of the predicted surface profile which is rolling speed dependent (dash-dot-dot line) to that rolling that is speed independent (dotted line)

and area of exit cross section of workpiece in oval-round (or round-oval) pass rolling sequence has been improved by employing rolling speed dependent spread model, established from a four-pass high speed rod rolling test. The validity of the model was examined by applying it to POSCO No. 3 Rod Mill. The conclusions may be summarized as follows:

1) The prediction methodology employed in this study was proven valid and reduced the computational time drastically. The model also showed a reasonable accuracy when it was applied to a rod mill where the rolling speed is very high.

2) The analytical method with a non-iterative computational frame is reliable and accurate. Hence it may become a valuable tool for the on-line control and the initial pass schedule design for a continuous rod rolling process. However, further studies seem necessary to insure the validity of the model for diverse process conditions. For example, the effect of the material, temperature and friction on the surface profile should be investigated.

ACKNOWLEDGEMENT

This research was supported by the Chung-Ang University Research Grants in 2005.

REFERENCES

1. Park, J. J. and Oh, S. I., "Application of three-dimensional finite element analysis to shape rolling processes," ASME Trans, Journal of Engineering for Industry, Vol. 112, pp. 36-46, 1990.

2. Karhausen, K., Kopp, K. and De Souza, M. M., "Numerical simulation method for designing thermomechanical treatments, illustrated by bar rolling," Scandinavian Journal of Metallurgy, Vol. 20, No.6, pp. 351-363, 1991.

3. Shin, W., Lee, S. M., Shivpuri, R. and Altan, T., "Finite-slab element investigation of square-to-round multi-pass shape rolling," Journal of Materials Processing Technology, Vol. 2, No.1, pp. 141-154, 1992.

4. Komori, K., "Simulation of deformation and temperature in multi-pass caliber rolling," Journal of Materials Processing Technology, Vol. 71, No.2, pp. 329-336, 1997.

5. Kim, H. J., Kim, T. H. and Hwang, S. M., "A New Free Surface Scheme for Analysis of Plastic Deformation in Shape Rolling," Journal of Materials Processing Technology, Vol. 2, No.1, pp. 81-93, 2000.

6. Shinokura, T. and Takai, K. A., "A New method for calculating spread in rod rolling," Proceeding of experimental verification of process models, ASM, Cincinati, USA, pp. 175-188, 1983.

7. Lee, Y. and Choi, S., "New Approach for the Prediction of Stress Free Surface Profile of Workpiece in Rod Rolling," ISIJ International, Vol. 40, No.6, pp. 624-626, 2000.

8. Lee, Y. and Goldhahn, G., "Prediction Model of the Exit Cross Sectional Shape in Round-Oval-Round Pass Rolling," Int. J. Korean Society of Precision Engineering, Vol. 2, No.1, pp. 87-93, 2001.